Development 133, 4257-4267 (2006) doi:10.1242/dev.02588

Compartmentalisation of Rho regulators directs cell invagination during tissue morphogenesis

Sérgio Simões[1,2], Barry Denholm[3], Dulce Azevedo[1], Sol Sotillos[4], Paul Martin[5], Helen Skaer[3], James Castelli-Gair Hombría[4] and António Jacinto[1,2,*]

During development, small RhoGTPases control the precise cell shape changes and movements that underlie morphogenesis. Their activity must be tightly regulated in time and space, but little is known about how Rho regulators (RhoGEFs and RhoGAPs) perform this function in the embryo. Taking advantage of a new probe that allows the visualisation of small RhoGTPase activity in *Drosophila*, we present evidence that Rho1 is apically activated and essential for epithelial cell invagination, a common morphogenetic movement during embryogenesis. In the posterior spiracles of the fly embryo, this asymmetric activation is achieved by at least two mechanisms: the apical enrichment of Rho1; and the opposing distribution of Rho activators and inhibitors to distinct compartments of the cell membrane. At least two Rho1 activators, RhoGEF2 and RhoGEF64C are localised apically, whereas the Rho inhibitor RhoGAP Cv-c localises at the basolateral membrane. Furthermore, the mRNA of RhoGEF64C is also apically enriched, depending on signals present within its open reading frame, suggesting that apical transport of RhoGEF mRNA followed by local translation is a mechanism to spatially restrict Rho1 activity during epithelial cell invagination.

KEY WORDS: Cell invagination, Myosin II, Actin cytoskeleton, Small GTPase Rho1, RhoGEFs, RhoGAPs, Posterior spiracles, *Drosophila*

INTRODUCTION

Small GTPases of the Rho subfamily work as regulatory switches and play essential roles in Actin cytoskeleton organisation, cell:cell adhesion, cell:substrate adhesion, cell polarity, cytokinesis, cell cycle progression and cell migration. The Rho subfamily of genes is highly conserved in evolution and comprises three major members, Rho, Rac and Cdc42, which cycle between an active GTP-bound and an inactive GDP-bound state (Jaffe and Hall, 2005; Symons and Settleman, 2000). The GTPase switch GTP/GDP is determined by the action of two main classes of regulatory proteins: the Guanine nucleotide exchange factors (GEFs), which act as GTPase activators by releasing GDP and allowing its replacement by GTP (Rossman et al., 2005), and the GTPase activating proteins (GAPs), which promote the GTPase inactive state by stimulating its GTP hydrolysing capacity (Moon and Zheng, 2003).

Spatial and temporal restriction of small RhoGTPase activity inside a cell is fundamental, for example, to the regulation of movements and cell-cell contacts that are required for morphogenesis. During the formation of epithelia, Rac and Cdc42 are specifically recruited to the cadherin-cadherin contact sites formed between neighbouring cells, where they drive the formation of filopodia and/or lamellipodia that will contribute to generate intimate cell-cell contacts (Braga, 2000). Another example of spatially restricted RhoGTPase activity has been found during migration of single cells, in which Rac-GTP accumulates at higher levels at the leading edge (Kraynov et al., 2000), where it induces Actin polymerisation and integrin adhesion complex assembly.

[1]Instituto de Medicina Molecular, Faculdade de Medicina de Lisboa, Portugal. [2]Instituto Gulbenkian de Ciência, Oeiras, Portugal. [3]Department of Zoology, University of Cambridge, Downing Street, Cambridge CB2 3EJ, UK. [4]Centro Andaluz de Biología del Desarrollo, Universidad Pablo de Olavide, Sevilla, Spain. [5]Department of Physiology, School of Medical Sciences, University of Bristol, University Walk, Bristol BS8 1TD, UK.

*Author for correspondence (e-mail: ajacinto@fm.ul.pt)

Accepted 18 August 2006

Evidence that the spatial and temporal control of small RhoGTPase function must be correlated with the activity of Rho regulators during tissue morphogenesis is suggested from studies on cell shape changes occurring during gastrulation and neurulation. In *Drosophila* gastrulation, a secreted factor Folded gastrulation (Costa et al., 1994) initiates a signal through interaction with a G protein-coupled receptor (still unknown) and a heterotrimeric G protein α subunit, Concertina (Parks and Wieschaus, 1991) to activate DRhoGEF2, the small GTPase Rho1 and subsequently Myosin II (Barrett et al., 1997; Nikolaidou and Barrett, 2004). This pathway is essential to induce constriction of the apical surface of mesodermal cells, leading to their invagination. In vertebrates, apical constriction of neuroepithelial cells, mediated by reorganisation of the Actin cytoskeleton, contributes to closure of the anterior neural tube. Interestingly, mice mutant for p190 RhoGAP show defects in anterior neural tube closure, due to failure in apical constriction and in intracellular re-organisation of the Actin cytoskeleton of neuroepithelial cells (Brouns et al., 2000). Together, these observations suggest that Rho acts apically during constriction of (neuro)epithelial cells and its function is tightly regulated by RhoGEF and RhoGAP activities.

Despite this, it is still unclear how spatially localised activation of small RhoGTPases is achieved and, with few exceptions (Bement et al., 2005), no tools exist that allow the direct visualisation of their activity during embryonic development. Additionally, little is known about how Rho regulators spatially and temporally control their targets in vivo, during the complex morphogenetic movements that shape the embryo.

Cell invagination is a widespread movement during embryogenesis and it is commonly dependent on Rho function (Pilot and Lecuit, 2005). Using the posterior spiracles of the *Drosophila* embryo as a model, we show that apically localised Myosin II and Rho1 are essential to control this morphogenetic movement. By expressing a GFP-based probe that allows the visualisation of active Rho1, we present evidence that during cell invagination this RhoGTPase is exclusively activated on the apical membrane of epithelial cells. Correlating with this local activation, we found that

two Rho1 activators (RhoGEF2 and RhoGEF64C) are upregulated and localise apically in the invaginating cells, while a Rho1 inhibitor, the RhoGAP Cv-c (Crossveinless-c), occupies the complementary basolateral membrane domain. This differential distribution of Rho regulators is required for the correct function of Rho1, which drives invagination of epithelial cells.

MATERIALS AND METHODS

Fly strains and genetics

The following fly strains were used: yw; ubi-DE-Cad-GFP (Oda and Tsukita, 2001); *Sqh^{AX3}*; ubi-Sqh-GFP (Royou et al., 2002); ems-GAL4 (Merabet et al., 2002); UAS-αCat-GFP (Oda and Tsukita, 1999); UAS-GFP-Actin (Verkhusha et al., 1999); UAS-mRFP-Actin#30 (this study); UAS-GFP (Bloomington Stock Center); UAS-RhoN19 (Strutt et al., 1997); UAS-PNKG58AeGFP (this study); UAS-RhoV14 (Fanto et al., 2000); UAS-RacN17 (Luo et al., 1994); UAS-DRhoGEF64C FL and UAS-DRhoGEF64CΔDbl (Bashaw et al., 2001); UAS-GEF64CΔ5′3′UTR (this study); UAS-Cv-c (Denholm et al., 2005); UAS-Venus-Cv-c-93 (this study); *rho1^{1B}*/CyO (Magie and Parkhurst, 2005); *rho1^{72R}*/CyO (Strutt et al., 1997); RpII140^{wimp}/TM3 Sb^{1} (Bloomington Stock Center); *gef64C^{1}*/TM3 and *gef64C^{29}*/TM3 (Bashaw et al., 2001); P[FRT(w^{hs})]G13 *DRhoGEF2$^{I(2)04291}$*/CyO (Hacker and Perrimon, 1998); yw P[FRT(w^{hs})]101 *sqh^{1}*/FM7 (Karess et al., 1991); *cv-c^{7}*/TM3 (Denholm et al., 2005).

Germline clones of DRhoGEF2$^{I(2)04291}$ and *sqh^{1}* were generated using the FLP-DFS system (Chou and Perrimon, 1996). yw P[FRT(w^{hs})]101 *sqh^{1}*/w* P[FRT(w^{hs})]101 ovo^{D1} females carrying germline clones were crossed with w; ems-GAL4 UAS-GFP-Actin males. Maternal and zygotic mutants for *rho1^{1B}* were generated using the *wimp* strategy (Magie et al., 1999).

Live imaging

Embryos expressing ubi-DE-CadGFP or GFP-Actin with the ems-GAL4 driver were prepared for live imaging and analysed as described (Woolner et al., 2005).

Molecular biology and transgenic lines

To express PKNG58AeGFP, we generated pUAST-PKNG58AeGFP. The N-terminus of *Drosophila* PKN (first 339 amino acids), including the point mutation G58A, was PCR amplified from pCasperPKNG58A (kind gift from Jeffrey Settleman). This PCR fragment was cloned into the *Eco*RI/*Xba*I sites of pUAST (Brand and Perrimon, 1993). Next, eGFP was PCR amplified from pEGFP-N1 (Clontech) and cloned into the *Xba*I site of the previous construct.

Venus-Cv-c was generated by cloning the full-length cDNA of cv-c (Denholm et al., 2005) into the pENTR directional TOPO cloning vector (pENTR/D) and subsequently transferred into pTVW (UASt promoter, N-terminal Venus tag – obtained from DGRC) using the Gateway technology (Invitrogen).

mRFP-Actin was made by fusing the 700 bp fragment of mRFP (Campbell et al., 2002) with 1100 bp of *Drosophila* Actin 5c, and cloned into pUAST.

pUAST-RhoGEF64CΔ5′3′UTR was obtained by digestion of pUASTGEF64C FL (Bashaw et al., 2001) with *Eco*RI and *Nhe*I and subcloning the resulting fragment into pUAST. Transgenic flies were generated using standard procedures.

S2 cell culture, RNAi and transfection

Drosophila Schneider S2 cells were cultured and RNAi was performed according to Clemens et al. and Schneider (Clemens et al., 2000; Schneider, 1972). Templates for in vitro transcription of *Rho1* were generated as described below for *RhoGEF64C*, and contained 527 bp from position 655 (CG8416-RC). Expression of PKNG58AeGFP in S2 cells was obtained by co-transfection of 20 ng of pUAST-PKNG58AeGFP with 100 ng of pAc5.1/V5-HisB-GAL4 in six well plates. In some cases, 100 ng of the active forms RhoV14, RacV12, Cdc42V12 or for the dominant-negative, RhoN19, RacN17 or Cdc42N17 cloned in pUAST were also co-transfected by using the CellFectin method according to the manufacturer's specifications (Invitrogen Life Technologies).

GTPase-binding assays

S2 cell extracts expressing PKNG58AeGFP were prepared 24 hours post-transfection, in lysis buffer [50 mmol/l Tris (pH 7.8), 150 mmol/l NaCl, 1% Nonidet-40], and were precleared twice with protein A-Sepharose beads for 30 minutes (4°C). *Drosophila* Rho1, Rac1, Rac2 and Cdc42-GST proteins were prepared according to standard methods and pre-incubated with GDP or GTPγS according to (Lu and Settleman, 1999). GTPase binding to PKNG58AeGFP was next assayed by SDS-PAGE, followed by immunoblotting with an anti-GFP monoclonal antibody (Roche).

RNA interference in embryos

For the synthesis of dsRNA for *RhoGEF64C*, a region of 773 bp from position 1237 (CG32239-RA) was PCR amplified from genomic DNA with primer pairs containing the T7 promoter sequence at the 5′ end. The PCR products were used as templates for the T7 transcription reactions with the T7 Ribomax Large Scale Production Kit (Promega). The dsRNA was dissolved in injection buffer at a final concentration of 2.2 μg/μl and injected into 0- to 1-hour-old embryos derived from the cross between w; ems-GAL4 UAS-GFP-Actin females and yw males.

In situ hybridisation, immunohistochemistry and cuticle preparations

Whole-mount in situ hybridisation was carried out using standard methods (Lehmann and Tautz, 1994) with a digoxigenin-labelled probe generated by transcription of *DRhoGEF64C* (CG32239-RA) DNA region 1237-2010 (nucleotide positions).

For immunohistochemistry, embryos were dechorionated in commercial bleach, fixed in a 1:1 mix of formaldehyde 4% in PBS (Ca^{2+} free): n-heptane for 30 minutes at room temperature and hand devitellinised. The following primary antibodies were used: mouse anti-Armadillo (N2 7A1, Hybridoma Bank) 1:50; rabbit anti-GFP (AbCAM #290) 1:2000; mouse anti-Dlg (4F3, Hybridoma Bank) 1:250; mouse anti-α-Spectrin (3A9, Hybridoma Bank), 1:10; mouse anti-GEF64C (Bashaw et al., 2001) 1:50; rabbit anti-DRhoGEF2 (Padash Barmchi et al., 2005) 1:1000; rabbit anti-Myosin II heavy chain (Bloor and Kiehart, 2001) 1:500; mouse anti-Rho1 (P1D9) (Magie et al., 2002) 1:50 and Phalloidin Alexa-594 (Molecular Probes) 1:200. All dilutions were done in PBT (BSA 1% and Triton X-100 0.1% in PBS). Secondary antibodies were coupled to Alexa^{488} or Alexa^{594} (Molecular Probes), and diluted in PBT at 1:400. Cuticle preparations were done as described (Hu and Castelli-Gair, 1999).

RESULTS

Spiracle cell invagination involves apical constriction and basolateral membrane elongation

The posterior spiracles are the respiratory organ of the first instar *Drosophila* larva. They contain an internal multicellular tube, the spiracular chamber, which links the trachea to the exterior, allowing gas exchange. Formation of the spiracular chamber begins at stage 11 (7 hours after egg laying), when a group of ~70 epithelial cells localised posteriorly to the eighth abdominal tracheal pit start to invaginate into the embryo (Hu and Castelli-Gair, 1999). We studied spiracle cell behaviour during the invagination process by performing time-lapse analysis in live *Drosophila* embryos expressing DE-Cadherin fused to GFP (Oda and Tsukita, 2001). At stage 11, when the embryonic germ band is fully extended, the future spiracular chamber cells were still localised superficially and were indistinguishable from the neighbouring cells (Fig. 1A, *t*=0 minutes, see Movie S1 in the supplementary material and Fig. 1B, part i). As the germ band started to retract, the most anterior cells rearranged their relative positions around the tracheal opening (Fig. 1B, part ii, arrow) until they met, forming a lumen in continuity with the tracheal dorsal branch (Fig. 1B, part iii). During this rearrangement, all the cells in the spiracle primordium constricted apically, resulting in an inward depression of the tissue around the luminal opening (Fig. 1A, *t*=134 minutes). This invagination

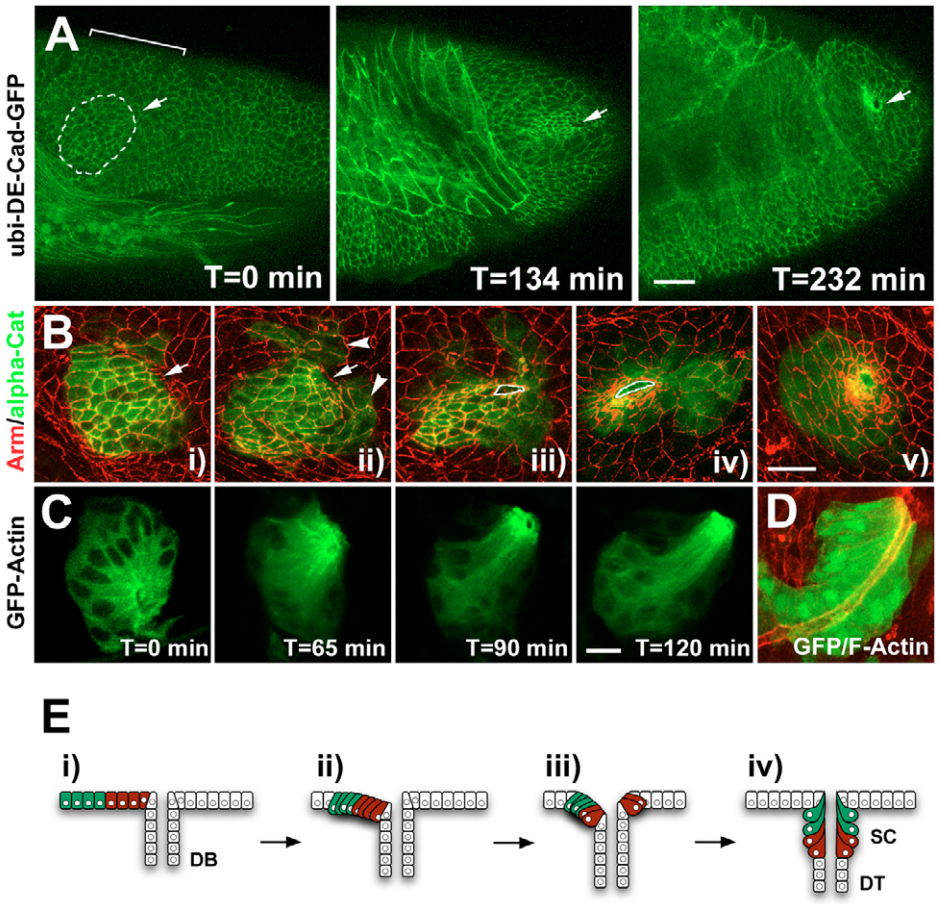

Fig. 1. Posterior spiracle cell invagination involves apical constriction and basolateral membrane elongation. (**A**) Stills of a movie showing the A8 segment (bracket) of a DE-Cad-GFP-expressing embryo. At stage 11 (*t*=0 minutes), spiracular chamber cells (dashed line) are superficial and localise posteriorly to the A8 tracheal pit (arrow). Later, notice apical constriction and inward cell movement to form a lumen (arrow). (**B**) Spiracle cells are expressing α-Catenin-GFP (green), using the ems-GAL4 driver (spiracle-specific); Armadillo (β-Catenin) is in red. All images are top views. (i,ii) Initial lumen formation (stage 11) involves rearrangement of the most anterior cells (arrowheads) around the tracheal opening (arrow). (iii) the more posterior cells (left from white outline) constrict apically and invaginate later (iv), to form the complete chamber (v). (**C**) Stills of a live embryo expressing GFP-Actin in the spiracle invaginating cells. *t*=0 minutes corresponds to end of stage 12. Notice apical enrichment of GFP-Actin and elongation of the basolateral cell domain, with the cell nuclei (black) remaining basally localised. (**D**) Phalloidin staining (red) in the spiracular chamber cells expressing GFP (green). Notice the accumulation of F-Actin at the apical/luminal side of the spiracular chamber cells (lateral view). (**E**) Diagram showing invagination of the posterior spiracle cells (lateral view). The cells belonging to the spiracle primordium (red and green) constrict apically (i,ii); the more anterior cells (red) rearrange around the A8 tracheal dorsal branch (DB) (iii) and invaginate first, occupying deeper positions in the spiracle. These are followed by the most posterior cells (green), which then occupy more superficial positions. The invaginated cells form a multicellular tube (spiracular chamber) in continuity with the tracheal dorsal trunk. During invagination, cells also elongate their basolateral membrane, acquiring a bottle shape (iv). Anterior is to the left in all panels; note that in the extended germ band stage (stage 11) the anterior cells are on the right side because the embryo is folded. Scale bars: 20 μm in A; 10 μm in B-D. DT, tracheal dorsal trunk; SC, spiracular chamber.

occurred in a spatially and temporally controlled manner, as the cells adjacent to the tracheal opening invaginated first (forming a lumen), followed in turn by the more distal (posterior) cells (Fig. 1B, parts iii,iv; see also the diagram in Fig. 1E). Apical constriction and ordered invagination continued until the end of germ band retraction, by which time all the spiracle chamber cells had invaginated into the embryo, forming a tube continuous with the trachea (Fig. 1A, *t*=232 minutes, Fig. 1B, part v, and Fig. 1D).

To visualise the Actin cytoskeleton during the invagination process, we expressed GFP-Actin in the spiracle invaginating cells and followed in vivo cell shape changes. GFP-Actin preferentially accumulated at the apical side of the invaginating cells, correlating with constriction at that side (Fig. 1C). In a fully developed spiracle, the luminal surface of the spiracular chamber was formed by the apical side of the invaginated cells, and was also lined by F-Actin, as revealed by Phalloidin staining (Fig. 1D). Simultaneously with apical constriction, the invaginating cells elongated up to fourfold at the opposite, basolateral, side, with the nucleus remaining basally localised. After stage 16, spiracle cells secrete a refractive cuticle, known as the Filzkörper, inside the luminal space, which works as a filter during larval breathing (Hu and Castelli-Gair, 1999) (Fig. 3A).

Myosin II is apically enriched and essential for spiracle invagination

Apical constriction and invagination of epithelial cells are generally linked to recruitment of both F-Actin and Myosin II to the apical side (Young et al., 1991). Using transgenic embryos expressing the regulatory light chain of Myosin II [MRLC, encoded by the *spaghetti squash* (*sqh*) gene] fused to GFP (Royou et al., 2002), or antibodies against the heavy chain of Myosin II (Zip), we confirmed that this Myosin was apically enriched in the cells forming the spiracular chamber (see Fig. S1A in the supplementary material, wild type). Furthermore, this enrichment correlated with the onset of apical constriction. At stage 11, before cell invagination started, Myosin II was distributed along the entire lateral membrane, co-localising with the basolateral marker Dlg (Discs large) (Fig. 2A, stage 11). As the spiracle cells began constricting apically, puncta of Myosin II appeared on their apical side (Fig. 2A, stage 12). At stage 13, when the entire primordium had invaginated, Myosin II was highly enriched apically, in a largely non-overlapping domain relative to Dlg (Fig. 2A, stage 13). This localisation, together with the observation that Actin also accumulates apically, co-localising with Myosin II, suggests that a contractile force based on Actin and Myosin II is acting during the process of invagination.

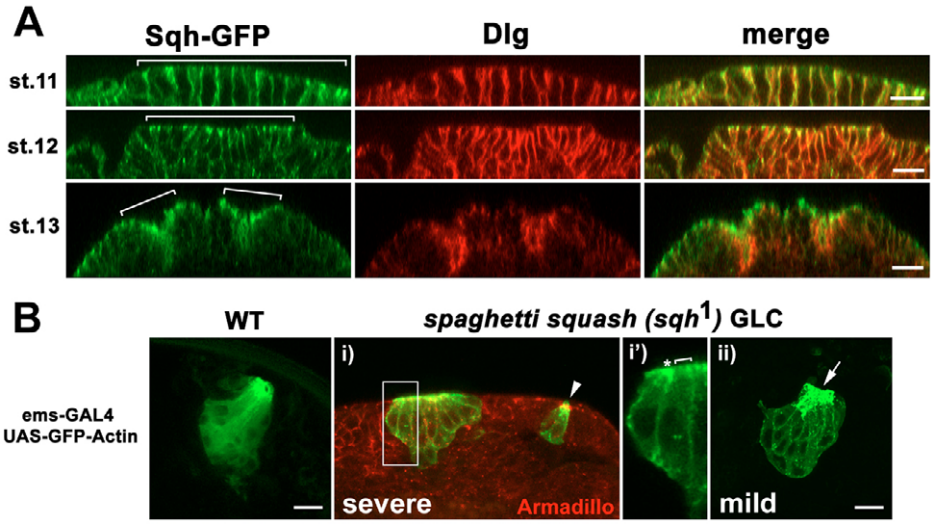

Fig. 2. Myosin II is apically enriched and essential for spiracle invagination. (**A**) Myosin II distribution is visualised in the spiracular chamber cells using embryos expressing Myosin II regulatory light chain (Spaghetti squash) fused to GFP (Sqh-GFP). Discs large (Dlg) (red) labels the basolateral membrane at stage 11/12 and only the lateral membrane at stage 13. The images are sagittal views and brackets indicate the position of the invaginating spiracle cells. Apical is up. (**B**) Spiracular chamber defects in sqh^{1GLC} embryos (i,ii) compared with wild type; spiracular chamber cells are labelled with GFP-Actin, using the ems-GAL4 driver. In i, spiracle cells remain on the surface of the embryo; the arrowhead indicates two spiracle cells detached from the main cluster; notice that some cells fail apical constriction (cell labelled with bracket in i′, which is a magnification of the rectangle in i), as opposed to other cells with a wedge shape and high accumulation of apical Actin (e.g. cell labelled with an asterisk). (ii) The arrow indicates the disrupted pattern of apical Actin in the mild class of sqh^{1GLC} spiracles. Scale bars: 10 μm.

To test this hypothesis, we analysed the morphology of the spiracular chamber in embryos with a strong reduction in the maternal and zygotic levels of MRLC, by making germline clones of a hypomorphic mutation in *sqh*, sqh^{1} (Karess et al., 1991). This mutation, as opposed to null mutations in Myosin II, does not abolish egg laying (Barros et al., 2003) and allows embryonic development to proceed beyond spiracle formation. Consistent with a role for apical Myosin II in exerting the driving force during cell invagination, spiracle cells failed to invaginate and to form a lumen in sqh^{1GLC} embryos (Fig. 2B, part i). In addition, clusters of cells were seen detached from the main group (Fig. 2B, part i, arrowhead), suggesting that Myosin II is also important in coordinating cellular movement during invagination. Although Actin was still apically enriched in most of the spiracle cells in these mutants, failure in apical constriction was occasionally observed (Fig. 2Bi′). Embryos that were rescued by the paternal contribution of MRLC exhibited a milder phenotype, in which spiracle cells were able to invaginate but failed to form a lumen, showing a disrupted apical Actin cytoskeleton (Fig. 2B, part ii, arrow; compare with wild type in Fig. 2B). These observations demonstrate that apical Myosin II, together with Actin, is essential to correctly drive epithelial cell invagination and lumen formation.

Rho1 is essential for epithelial cell invagination

The small GTPase Rho is known to promote Myosin II activity via Rho-Kinase (ROCK) activation, and to stimulate Actin polymerisation via Formin activation (Narumiya et al., 1997). Thus, apical enrichment of F-Actin and Myosin II during spiracle cell invagination suggests the involvement of *Drosophila* Rho1 in this process. To test this hypothesis, we analysed spiracle morphology in both zygotic and maternal/zygotic mutants for *Rho1*, using the *wimp* strategy (Magie et al., 1999). In both cases, a large majority of $Rho1^{1B}$ null embryos showed a dilated or irregular Filzkörper, especially at the most distal part of the tube, symptomatic of disrupted invagination (75.8% in zygotic $Rho1^{1B}$ mutants, n=116 and 69% in $Rho1^{1B}$ maternal/zygotic mutants, n=185) (Fig. 3B; compare with wild type, Fig. 3A). These defects correlated with a partial disruption of the cortical Actin cytoskeleton in the spiracular chamber of late embryos (Fig. 3D). Additionally, in these experiments about 4% of zygotic $Rho1^{1B}$ mutants and 13% of maternal/zygotic mutants showed a complete failure in spiracle cell invagination (Fig. 3C), with the Filzkörper forming on the surface of the embryo. These observations suggest that Rho1 activity is essential for proper epithelial cell invagination and tubulogenesis and controls the assembly of apical Actin during this process.

Similar results were obtained by spiracle-specific expression of a dominant negative Rho protein (RhoN19), which led to a block of the invagination process, causing the spiracle cells to remain on the surface of the embryo (Fig. 3E,F). These uninvaginated cells showed a disrupted cortical Actin cytoskeleton at their apical side, correlating with a non-uniform pattern of apical Myosin II (Fig. 3H, arrowhead; compare with wild type, Fig. 3G, and see Fig. S1A in the supplementary material). Nevertheless, as observed in *Rho1* mutants, elongation of the basolateral membrane could still be observed, indicating that Rho1 function is not required for this process (Fig. 3H, arrow). Knocking down Rho1 activity also affected the establishment of proper apical cell-cell adhesion, as assessed by the defects seen in the adherens junctions architecture (see Fig. S1B in the supplementary material).

Rho1 activity is apically restricted during spiracle cell invagination

Loss of Rho1 function led to apical but not basolateral defects in the invaginating spiracle cells, suggesting that the activity of this GTPase is required apically during such morphogenetic movement. This prediction is further supported by two lines of evidence. First, immunofluorescence against Rho1 protein revealed that, despite

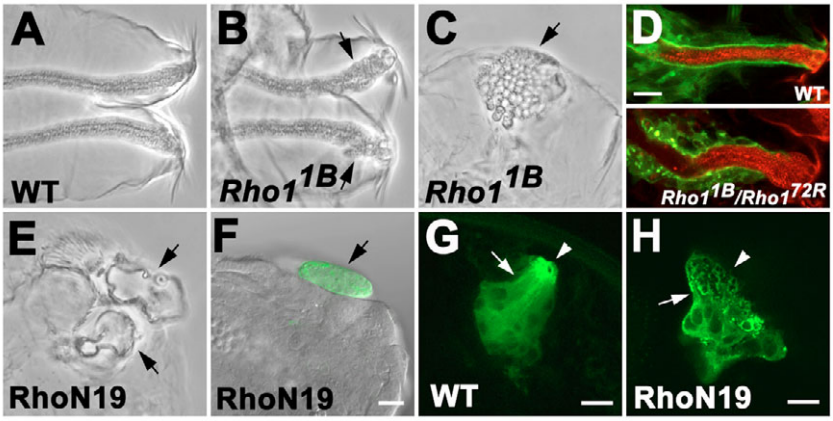

Fig. 3. Rho1 is essential for spiracle invagination. (**A**) Wild-type Filzkörpers. (**B**) Cuticle of a null mutant for *Rho1* (*Rho1*^{1B}) showing irregular Filzkörpers (arrows). (**C**) Severe class of *Rho1*^{1B} embryos, with one uninvaginated Filzkörper. (**D**) GFP-Actin (green) distribution in the spiracular chamber of wild type and *Rho1*^{1B}/*Rho1*^{72R} mutants (stage 17); red, Filzkörper autofluorescence obtained with the 488 nm laser. In wild-type spiracles, a continuous line of Actin surrounds the Filzkörper, while in late *Rho1* mutants this pattern is partially lost. (**E**,**F**) Expression of the dominant negative form of Rho1, RhoN19, impairs Filzkörper secretion (E) and the invagination of spiracle cells (F, arrow); green, GFP-Actin. (**G**,**H**) Wild-type spiracle and a spiracle in which RhoN19 has been expressed visualised with GFP-Actin. Expression of RhoN19 disrupts the accumulation of apical Actin (arrowhead), while elongation of the basolateral membrane is still observed (arrow). Scale bars: 10 μm.

being ubiquitous, Rho1 was strongly enriched on the apical side of the invaginating spiracle cells, surrounding the lumen of the spiracular chamber (Fig. 4A, parts i,ii). Second, we developed a GFP-based probe (herein termed PKNG58AeGFP), which recognizes the active, GTP-bound form of Rho1 and that can be expressed in vivo using the UAS/GAL4 system (see Fig. S2 in the supplementary material). To follow Rho1 activation and, simultaneously, Actin distribution, during invagination and tube formation, we expressed this probe together with mRFP-Actin in the spiracle cells. At stage 11, before the onset of epithelial cell invagination, PKNG58AeGFP appeared diffuse throughout the spiracle primordium (Fig. 4B, early stage 11). Slightly later, a distinct accumulation of the GFP signal was seen in the first invaginating cells adjacent to the last tracheal pit, and this was accompanied by a higher accumulation of mRFP-Actin in these cells (Fig. 4B, late stage 11). During apical constriction and spiracle cell elongation, our probe accumulated exclusively at the most apical side of the invaginating cells, where mRFP-Actin was also found (Fig. 4B, b.c.). After invagination, PKNG58AeGFP and mRFP-Actin were still detected apically, surrounding the lumen of the spiracular chamber (Fig. 4B, stage 13 and stage 17). Similar results were observed using six independent transgenic lines of UAS-PKNG58AeGFP, without any obvious phenotypic defects in spiracle morphogenesis.

To study the functional relevance of restricting Rho1 activity to the apical membrane during cell invagination, we analysed the effects of activating this GTPase in a spatially unrestricted manner, by overexpressing the constitutively activated form of Rho1, RhoV14, using the spiracle driver ems-GAL4. Simultaneous expression of our PKNG58AeGFP probe confirmed that Rho1 activity was ectopically detected throughout the entire plasma membrane upon expression of this activated form of Rho1 (Fig. 4C, part i; compare with wild-type control, Fig. 4C, left panel). Unrestricted Rho1 activation led to obvious defects in spiracle cell shape and localisation in late embryos: clusters of mini-bottle-shaped cells were seen superficially localised, indicating that ectopic Rho1 activation blocks spiracle cell invagination and inhibits the elongation of their basolateral membranes (Fig. 4C, part ii; compare with wild-type control in Fig. 3G). These RhoV14-expressing cells could still apically constrict and accumulate higher amounts of GFP-Actin on their apical side, probably due to the additive effect of the endogenous Rho1. Nevertheless, they failed to form a lumen, as assessed by the very disorganised and superficially localised Filzkörpers (Fig. 4C, part iii). We conclude that wild-type spiracle cell elongation and correct invagination/lumen formation require Rho1 to be active exclusively on the apical membrane.

RhoGEF64C mRNA and protein are apically localised in the spiracle cells

To further understand the mechanism by which Rho1 activity is apically restricted, we searched for Rho activators that are expressed during spiracle invagination. We found that *RhoGEF64C*, previously described to regulate Rho1 in the embryonic central nervous system (Bashaw et al., 2001), was specifically expressed by the invaginating spiracle cells from early stage 12 until the spiracular chamber was fully formed (Fig. 5A). This RhoGEF is also present in other multicellular tubes, including the salivary glands, foregut and hindgut and at low levels in the epidermis.

Immunostaining of RhoGEF64C with a specific monoclonal antibody (Bashaw et al., 2001) showed that this RhoGEF localised apically, overlapping with the polymerised F-Actin surrounding the lumen of the spiracular chamber (Fig. 5B). Strikingly, we observed that *RhoGEF64C* mRNA was also apically enriched in the invaginating spiracle cells (Fig. 5C) and in the hindgut (Fig. 5D), indicating that this mRNA can be apically transported in epithelial cells. These observations suggest the possibility that RhoGEF64C activity is spatially controlled by apical targeting of its mRNA, followed by local translation.

To find the sequence elements responsible for the apical localization of *RhoGEF64C* mRNA, we overexpressed several truncations of RhoGEF64C cDNA in the posterior spiracles and assessed for mRNA localisation. Neither truncating the 5′UTR alone (UAS-RhoGEF64C FL, full length) (Bashaw et al., 2001) nor both the 5′UTR and the 3′UTR (UAS-RhoGEF64C Δ5′3′UTR) affected the apical localisation of RhoGEF64C mRNA. However, a deletion of 1.8 kb from the 3′ region, including

the 3′UTR, the Dbl domain (Rho interacting domain) and a putative PH domain (Pleckstrin Homology) (UAS-RhoGEF64CΔDbl) (Bashaw et al., 2001), disrupted apical mRNA localisation in the posterior spiracles (Fig. 5E). We conclude that the apical localising element(s) of RhoGEF64C mRNA are situated within the C-terminal coding region, which includes the Dbl and PH domains of this RhoGEF.

RhoGEF64C and RhoGEF2 promote apical Rho1 activity during the formation of the spiracular chamber

The apical localisation of RhoGEF64C makes it a good candidate for regulating Rho1 in a polarised manner during invagination. To test this, we co-expressed RhoGEF64C (UAS-RhoGEF64C FL) and the dominant negative form of Rho1, RhoN19, in the spiracle cells.

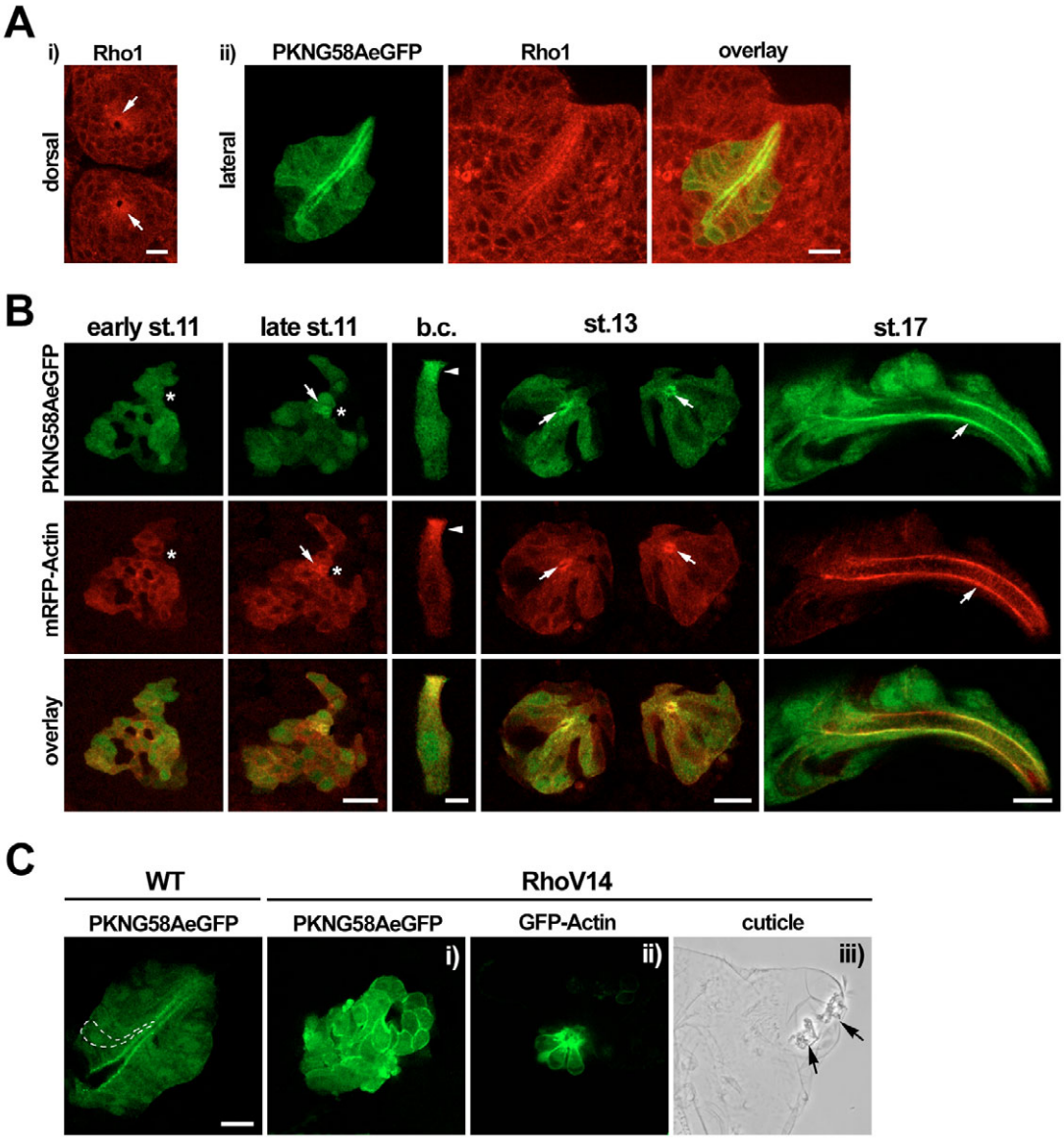

Fig. 4. Rho1 activity is apically restricted during spiracular chamber formation. (**A**) Immunofluorescence against Rho1 protein showing its apical accumulation around the lumen of the spiracular chamber (arrows); (i) dorsal view and (ii) lateral view. (ii) The PKNG58AeGFP probe overlaps with apical Rho1, reflecting the local activation of this RhoGTPase. (**B**) Rho1 activity during formation of the spiracular chamber. Spiracle cells co-expressing PKNG58AeGFP and mRFP-Actin. *early st11* – low levels of PKNG58AeGFP are detected throughout the spiracle primodium. The asterisk indicates the A8 tracheal pit position. Anterior is to the right; *late st11* – the onset of Rho1 activity is detected in the first invaginating cells (arrow) localised posteriorly to the last tracheal pit. Notice also the higher accumulation of mRFP-Actin in these cells; *b.c.* – single invaginating bottle-shaped cell showing apical activation of Rho1 (arrowhead), which overlaps with apical accumulation of mRFP-Actin (apical is up); *stage 13* and *stage 17* – transverse and lateral views, respectively, of spiracular chambers showing accumulation of Rho1-GTP and mRFP-Actin at the luminal/apical surface (arrows). (**C**) Ectopic Rho1 activation blocks basolateral elongation and impairs cell invagination. The left panel shows active Rho1 (PKNG58AeGFP fluorescence) around the lumen of a wild-type spiracle (lateral view, stage 14); the dashed line outlines a single invaginated cell. The two middle panels represent spiracle cells co-expressing RhoV14 and PKNG58AeGFP (i) or GFP-Actin (ii). The right panel (iii) shows the Filzkorper defects (arrows) caused by the expression of RhoV14 (cuticle). In i, ectopic Rho1 activation is detectable on the cell membranes, as opposed to the apically restricted pattern in the wild type (same confocal settings as the WT control). ii shows a cluster of three spiracle cells with a mini-bottle shape, due to inhibition of basolateral elongation (compare with wild-type control, Fig. 3G). Scale bars: 10 μm, except B b.c, 3 μm.

This dominant negative mutant is expected to interfere with Rho1 function by sequestering its specific RhoGEFs. Accordingly, the expression of the apical RhoGEF64C was able to rescue the invagination defects caused by RhoN19, allowing the formation of normal spiracular chambers (73.8%, *n*=157) (compare Fig. 5F with Fig. 3E). By contrast, the truncated version, which lacked the Rho interacting domain (Dbl domain) and failed to localize apically, RhoGEF64CΔDbl, did not revert the RhoN19 phenotype. We conclude that RhoGEF64C acts as a Rho1 activator during the formation of the spiracular chamber.

To further investigate the function of RhoGEF64C in controlling Rho1 activity, we eliminated *RhoGEF64C* function by RNAi, injecting dsRNA for this RhoGEF into syncitial embryos carrying the transgenes ems-GAL4 (spiracle-specific) and UAS-GFP-Actin. Spiracle cells in RhoGEF64C RNAi embryos underwent normal invagination and lumen formation; however, at stage 17, these embryos showed an irregular Filzkörper, which correlated with a mild disruption of the cortical Actin cytoskeleton lining the lumen of the spiracular chamber (55%, *n*=126) (Fig. 5G). These defects are compatible with a partial loss of Rho1 activity (compare with *Rho1* zygotic mutants, Fig. 3D) and were similarly found in homozygous embryos for the null alleles *Rhogef64C*^{1} and *Rhogef64C*^{29} (Bashaw et al., 2001) (data not shown).

As the loss of function of *RhoGEF64C* did not cause invagination defects, as observed after the complete loss of Rho1 activity, we predicted that other RhoGEF(s) could be acting together with RhoGEF64C to activate Rho1 apically. A probable candidate is the ubiquitous and apically localised RhoGEF2, which is Rho1-specific and regulates epithelial cell invagination during development (Nikolaidou and Barrett, 2004; Padash Barmchi et al., 2005). We confirmed the expression and found an apical enrichment of DRhoGEF2 before and during invagination of the spiracle cells, overlapping with apical Actin (Fig. 6B and see Fig. S3 in the supplementary material). Furthermore, 34% of maternal and zygotic mutants for the null allele *DRhoGEF2*$^{l(2)04291}$ (DRhoGEF2 MZ) (Hacker and Perrimon, 1998) failed spiracle invagination, 26% presented lumen defects and 3.5% showed both defects (*n*=201) (see Fig. S3 in the supplementary material). DRhoGEF2 MZ embryos that were also heterozygous or homozygous (1:1) for the *Rhogef64C*^{1} null allele showed a mild increase in the frequency of spiracle defects (invagination defects, 31%; lumen defects, 35%; both defects, 8%; *n*=86). Taken together, these results show that at least two apical RhoGEFs, RhoGEF2 and RhoGEF64C, contribute to activate Rho1 apically during spiracle cell invagination.

RhoGAP Cv-c is localised basolaterally and is required for proper apical Rho1 activity

One emerging theme in small Rho GTPase regulation studies is that cycling between their GTP- and GDP-bound states might be required for effective signal flow in order to elicit downstream biological functions (Moon and Zheng, 2003). RhoGAPs are important players in this balance, as they accelerate the return of

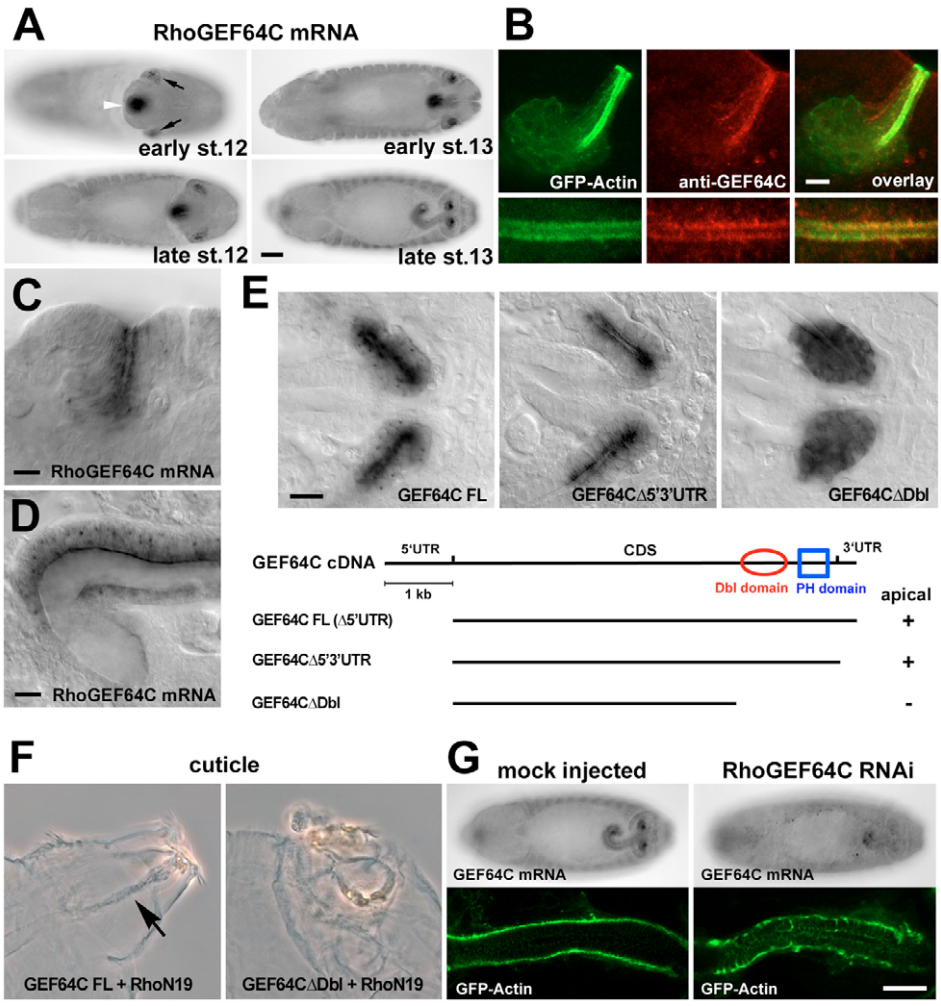

Fig. 5. RhoGEF64C is a positive regulator of Rho1 and its mRNA and protein are apically localised. (**A**) In situ hybridisation for *RhoGEF64C* showing expression in the posterior spiracle primordium (black arrows) and hindgut (white arrowhead), during retraction of the germ band. (**B**) Staining for the apical RhoGEF64C (red) in GFP-Actin expressing spiracle cells (stage 15). (**C**,**D**) *RhoGEF64C* mRNA is apically localised, surrounding the lumen of the posterior spiracles (C, lateral view) and hindgut (D, dorsal view) (stage 15). (**E**) Deletion of the Dbl plus PH domain (GEF64CΔDbl) abrogates apical localisation of RhoGEF64C mRNA in the posterior spiracles, as opposed to truncations of the UTR regions (GEF64C FL (Δ5′UTR) and GEF64C Δ5′3′UTR); CDS – coding sequence. Dorsal views. (**F**) Expression of RhoGEF64C FL rescues the RhoN19-induced phenotype, as opposed to the truncated form RhoGEF64CΔDbl. (**G**) *RhoGEF64C* RNAi downregulates the expression of this gene, as assessed by in situ hybridisation. Notice the formation of irregular Filzkörpers with partially disrupted cortical Actin. Green, GFP-Actin. Scale bars: 50 μm in A; 10 μm in B-D,F,G; and 20 μm in E.

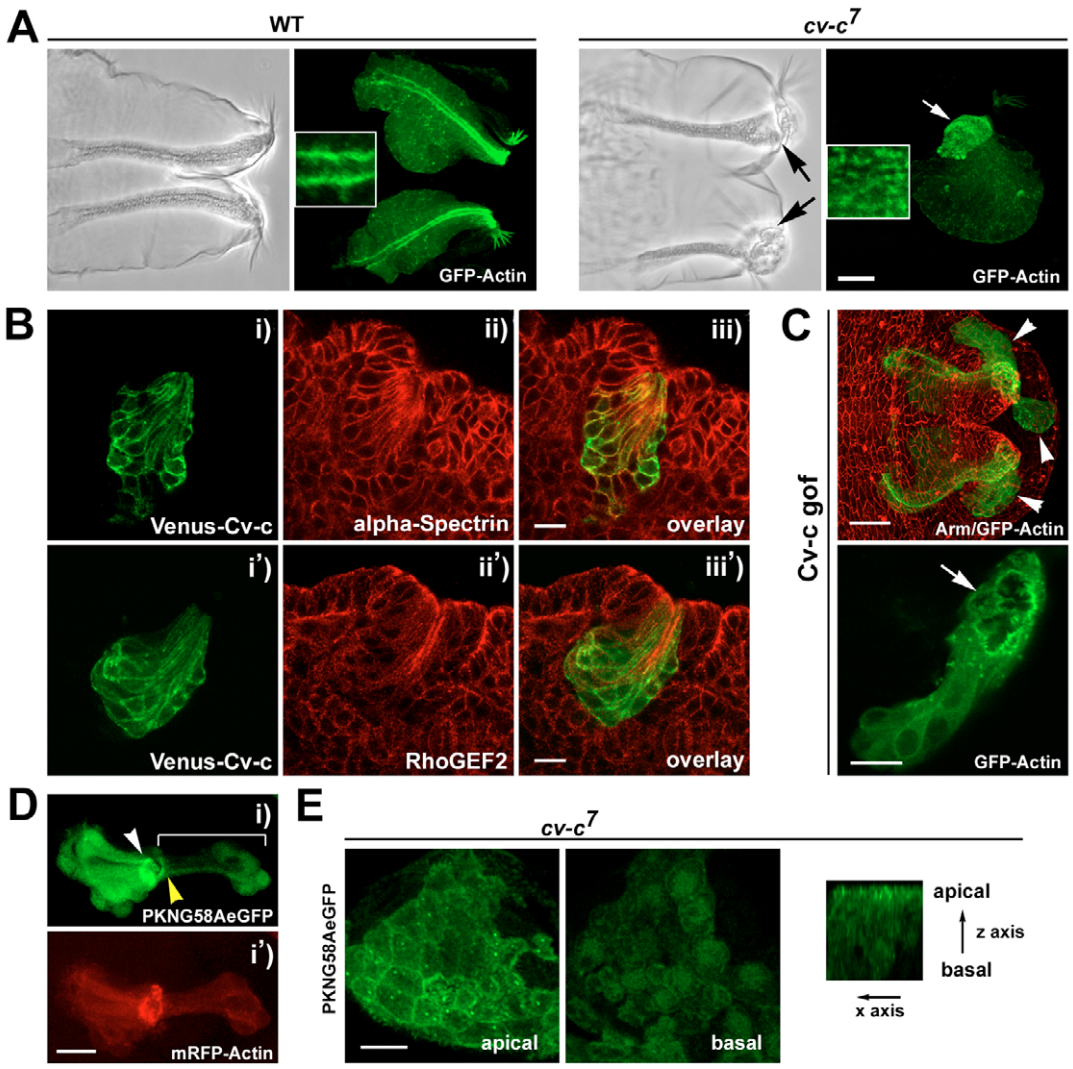

Fig. 6. RhoGAP Cv-c is localised basolaterally and controls Rho1 activity. (**A**) Cuticles and distribution of GFP-Actin (green) in the spiracles of wild-type and *cv-c*^{7} mutant embryos. Notice the partially uninvaginated Filzkörpers in *cv-c*^{7} mutants (arrows) accompanied by disruption of the apical Actin (inset). (**B**) Expression of Venus-Cv-c (green) in spiracle cells using the ems-GAL4 driver, co-stained with the basolateral marker α-Spectrin (red) (i-iii) and with RhoGEF2 (red) (i′-iii′). (**C**) Cv-c gain of function (using emsGAL4 and UAS-Cv-c) leads to invagination failure of the most distal cells of the spiracular chamber (arrowheads) correlating with a disruption of their apical Actin (arrow). Green, GFP-Actin; red, Armadillo. (**D**) PKNG58AeGFP (i) and mRFP-Actin (i′) profiles in spiracles overexpressing RhoGAP Cv-c. The cell cluster on the right (bracket) failed invagination and shows weaker apical Rho1 activity (yellow arrowhead) than the remaining invaginated cells (white arrowhead). (**E**) PKNG58AeGFP expression in a *cv-c*^{7} mutant spiracle with a severe phenotype. Apical and basal sections (dorsal view) and probe distribution along the xz axis. Notice the apical restriction of active Rho1, non-uniformly associated with the apical junctions. Scale bars: 10 μm.

RhoGTPases to their inactive state, and thus may act as positive regulators of Rho function (Symons and Settleman, 2000). Consistent with this view, previous work has implicated the RhoGAP Cv-c in spiracle cell invagination (Denholm et al., 2005). Zygotic *cv-c* mutants (*cv-c*^{7}) showed partial or complete invagination defects in their posterior spiracles, with a strongly disorganised pattern of apical Actin (Fig. 6A). As the vertebrate homologues of *cv-c*, p122/DLC-1 and DLC-2, were shown to act on RhoA, the mammalian homologue of *Drosophila* Rho1 (Leung et al., 2005; Wong et al., 2003), we hypothesised that Cv-c could also regulate Rho1 cycling during spiracle morphogenesis.

To determine the intracellular localisation of Cv-c, and compare it with the above-described RhoGEFs, we fused Cv-c to the modified YFP, Venus, and expressed this fusion in the spiracular chamber cells. Interestingly, and opposed to the exclusive apical localisation of the two RhoGEFs described above, RhoGAP Cv-c mainly localised to the basolateral membrane, overlapping with the basolateral marker α-Spectrin (Fig. 6Bi-iii). Double labelling of RhoGEF2 and Cv-c confirmed that these two classes of Rho regulators essentially occupied non-overlapping domains in the membrane of the invaginating cells, the apical and basolateral domains, respectively (Fig. 6Bi′-iii′).

To test whether Cv-c controls Rho1 activity during cell invagination, we overexpressed this RhoGAP in the spiracle cells. An increased expression of a RhoGAP is expected to downregulate the activity of the target RhoGTPase(s), thus mimicking the phenotype produced by the expression of their dominant negative forms. Gain of function of Cv-c [using UAS-Cv-c (Denholm et al., 2005)] caused

phenotypic defects similar to Rho1 loss of function (Rho1 mutants and UAS-RhoN19), but not to Rac loss of function (UAS-RacN17, see also Fig. S1B in the supplementary material): irregular Filzkörpers at the distal end and partially uninvaginated spiracles (compare Fig. 6C with wild type in Fig. S1B in the supplementary material). Frequently, the distal cells of the spiracular chamber failed to invaginate and showed decreased Rho1 activity, as confirmed by the lower levels of apical PKNG58AeGFP fluorescence (Fig. 6D). Furthermore, these cells maintained an elongated shape, but their apical Actin cytoskeleton was highly disrupted (Fig. 6C), in a manner similar to that observed upon expression of RhoN19 (Fig. 3H). Expression of stronger transgenic lines of UAS-Venus-Cv-c led to completely uninvaginated spiracles and fully phenocopied the defects caused by RhoN19 (data not shown). Together, these results indicate that Cv-c acts as a Rho1-GAP, being mainly excluded from the apical membrane domain in which Rho1 is active.

To test whether Cv-c is excluding Rho1 activity from the basolateral membrane, we expressed the PKNG58AeGFP probe in the spiracles of *cv-c*^{7} mutants. In these embryos we did not observe an increase in PKNG58AeGFP fluorescence on the basolateral membrane (Fig. 6E, xz axis projection), nor defects on spiracle cell elongation (which would be indicative of basolateral Rho1 activation, as shown in Fig. 4C). This suggests that other factors in addition to Cv-c act to exclude active Rho1 from this membrane domain. However, *cv-c*^{7} mutants show a pattern of active Rho1 restricted to the apical junctions in a non-uniform manner and not covering the entire apical membrane (Fig. 6E), as opposed to the wild type, where active Rho1 is found uniformly associated with the apical membrane (Fig. 4B, stage 17). These observations suggest that the absence of this RhoGAP leads to lower levels of apical Rho1-GTP, which correlate with the defects seen in the apical Actin cytoskeleton.

DISCUSSION

In this work we address the contribution of Rho1 activity and its spatial control during morphogenesis, using the posterior spiracles of the *Drosophila* embryo as a model. The formation of this organ involves dramatic changes in epithelial cell shape, which are very common during cell invagination, namely constriction at the apical side and elongation of the basolateral cell domain. These two contrasting behaviours at opposite cell poles induce tissue invagination.

Using a probe that allows the visualisation of Rho1 activity in the course of normal development, we present evidence that this GTPase is active at the apical side during the process of cell invagination. In the spiracles Rho1 activity is essential to control this movement, similarly to that previously shown during *Drosophila* gastrulation, when mesodermal cells fail to invaginate after inhibition of Rho1 function (Barrett et al., 1997; Hacker and Perrimon, 1998). We also observed an apical enrichment of Myosin II, a possible target of activated Rho1, analogous to that reported in other tissues of the fly embryo where this type of movement occurs, such as the mesoderm and the salivary glands (Nikolaidou and Barrett, 2004). Inhibition of Rho1 activity results in a disorganised pattern of apical Myosin II and F-Actin in the spiracle cells. We suggest that concentration of active Rho1 at the apical side organises the Actin cytoskeleton and promotes high Myosin II accumulation/activity in this region, leading to a contractile Actin-Myosin based force to produce a wedge-shaped cell.

Our data show that spatial restriction of Rho1 activity is achieved by distinct mechanisms. First, albeit ubiquitous, Rho1 protein is strongly enriched on the apical side of the invaginating spiracle cells. Second, to ensure that this GTPase is active exclusively on that side of the cell, opposing Rho regulators are differentially distributed in two distinct membrane domains: two Rho activators, RhoGEF64C and RhoGEF2, are apically localised, whereas a Rho inhibitor, the RhoGAP Cv-c, occupies the complementary, basolateral domain. As we have shown, cell shape changes and inward cell movements driving invagination are impaired if Rho1 becomes activated in a spatially unrestricted manner. These observations stress the importance of finely tuning Rho1 localisation and activation during normal tissue morphogenesis.

Several mechanisms might be at work to achieve the specific localisation of the Rho regulators that direct cell invagination. In the case of RhoGEF64C we show that its mRNA and protein are apically localised, suggesting that apical transport of RhoGEF mRNA followed by local translation is a mechanism to activate Rho1 in a spatially restricted manner. Recent studies show that the mRNA of RhoA can also be transported and locally translated in the axons and growth cones of embryonic rat neurons, where RhoA controls growth cone collapse in response to Semaphorin 3A (Wu et al., 2005). This shows that intracellular mRNA transport of Rho GTPases and of their regulators may be an important mechanism to control spatial GTPase activation.

Loss of function of the RhoGEFs involved in spiracle invagination leads to variable apical defects, which are compatible with a partial loss of Rho1 function: knocking out RhoGEF64C resulted in a mild disruption of cortical Actin without blocking invagination, while the absence of RhoGEF2 could result in a complete failure of the invagination process. These results suggest that several RhoGEFs are required to properly activate Rho1 during spiracle cell movement and organ shaping.

One interesting observation from our studies is the fact that mutants for the RhoGAP Cv-c did not show ectopic activated Rho1 on the basolateral membrane where this RhoGAP was localised. Thus, several mechanisms must be at work to ensure that Rho1 activity is excluded from the basolateral domain during cell invagination: the presence of at least one RhoGAP on the basal

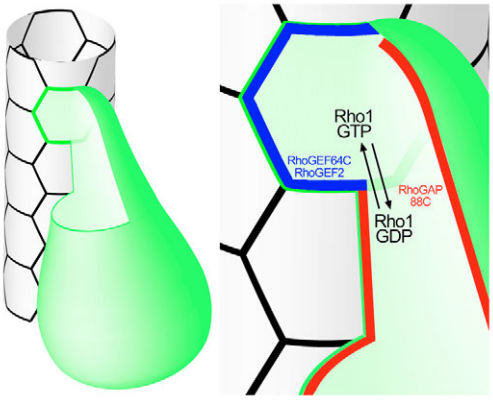

Fig. 7. Model for Rho1 activity during spiracle cell invagination and tube formation. Rho1 is exclusively active at the apical domain of the invaginating cells that form the spiracular chamber, by the action of RhoGEF2 and RhoGEF64C. At the apical side Rho1-GTP promotes Myosin II and F-Actin assembly/activity, being essential for correct cell invagination and lumen maintenance. Rho1 function is excluded from the basolateral domain both by the absence of RhoGEF activity and by the presence of the RhoGAP Cv-c. Inactivation of Rho1 at the basolateral domain is also required to maintain the steady state levels of apical Rho1-GTP.

membrane, the apical restriction of RhoGEFs and the existence of low levels of Rho1 protein on the basolateral side of the cells. In addition, we also observed that spiracles from severe *cv-c* mutants showed lower levels of apical Rho1-GTP than their wild-type counterparts, correlating with the disruption of their apical Actin. Defects in apical Actin/Myosin II were also reported during invagination of the tracheal pits in *cv-c* mutants (Brodu and Casanova, 2006). Taken together, these observations suggest that GTP hydrolysis is a necessary step in the regulation of Rho1 function during cell invagination and the RhoGAP Cv-c may help to maintain a steady state level of apical Rho1-GTP.

Based on the differential distribution of Rho1 GEFs and GAPs, we propose a model in which Rho1 must shuttle back and forth between two membrane compartments, being GTP-bound on the apical cell membrane and GDP-bound on the basolateral side (Fig. 7). Thus, during tissue morphogenesis, epithelial cells can couple their apical-basal polarity to the spatial control of small RhoGTPase function.

RhoGTPases act as dynamic switches in many developmental and cellular contexts. In order to understand how they orchestrate these dynamic processes, their activity states needs to be visualised over time. We anticipate that this work and the tools described will provide a basis for studying Rho1 activity in vivo. It will be interesting to extend this analysis to other contexts in which Rho GTPases are known to act – such a dorsal closure, neurulation, wound healing – and to identify the Rho regulators involved in each case, relating their spatial/temporal distribution with the patterns of Rho GTPase activity.

We thank Beatriz Garcia Fernandez, Isabel Campos, Evguenia Beckman, Rita Fior, Cristina Afonso and Domingos Henrique for helpful comments on the manuscript, and Udo Haecker, Greg Bashaw, Dan Kiehart, Steve Rogers, Andrea Brand, Susan Parkhurst and Jeffrey Settleman for reagents and fly stocks. This work was supported by grants from Fundação para a Ciência e Tecnologia, Portugal and European Union Framework Programme 6 (Network of Excellence Cells into Organs) to A.J. and by a grant from the Ministerio de Educación y Ciencia, Spain/FEDER BFU2004-1069 to J.H.

Supplementary material

Supplementary material for this article is available at http://dev.biologists.org/cgi/content/full/133/21/4257/DC1

References

Barrett, K., Leptin, M. and Settleman, J. (1997). The Rho GTPase and a putative RhoGEF mediate a signaling pathway for the cell shape changes in Drosophila gastrulation. *Cell* **91**, 905-915.

Barros, C. S., Phelps, C. B. and Brand, A. H. (2003). Drosophila nonmuscle myosin II promotes the asymmetric segregation of cell fate determinants by cortical exclusion rather than active transport. *Dev. Cell* **5**, 829-840.

Bashaw, G. J., Hu, H., Nobes, C. D. and Goodman, C. S. (2001). A novel Dbl family RhoGEF promotes Rho-dependent axon attraction to the central nervous system midline in Drosophila and overcomes Robo repulsion. *J. Cell Biol.* **155**, 1117-1122.

Bement, W. M., Benink, H. A. and von Dassow, G. (2005). A microtubule-dependent zone of active RhoA during cleavage plane specification. *J. Cell Biol.* **170**, 91-101.

Bloor, J. W. and Kiehart, D. P. (2001). zipper nonmuscle myosin-ii functions downstream of PS2 integrin in drosophila myogenesis and is necessary for myofibril formation. *Dev. Biol.* **239**, 215-228.

Braga, V. (2000). Epithelial cell shape: cadherins and small GTPases. *Exp. Cell Res.* **261**, 83-90.

Brand, A. H. and Perrimon, N. (1993). Targeted gene expression as a means of altering cell fates and generating dominant phenotypes. *Development* **118**, 401-415.

Brodu, V. and Casanova, J. (2006). The RhoGAP crossveinless-c links trachealess and EGFR signaling to cell shape remodeling in Drosophila tracheal invagination. *Genes Dev.* **20**, 1817-1828.

Brouns, M. R., Matheson, S. F., Hu, K. Q., Delalle, I., Caviness, V. S., Silver, J., Bronson, R. T. and Settleman, J. (2000). The adhesion signaling molecule p190 RhoGAP is required for morphogenetic processes in neural development. *Development* **127**, 4891-4903.

Campbell, R. E., Tour, O., Palmer, A. E., Steinbach, P. A., Baird, G. S., Zacharias, D. A. and Tsien, R. Y. (2002). A monomeric red fluorescent protein. *Proc. Natl. Acad. Sci. USA* **99**, 7877-7882.

Chou, T. B. and Perrimon, N. (1996). The autosomal FLP-DFS technique for generating germline mosaics in Drosophila melanogaster. *Genetics* **144**, 1673-1679.

Clemens, J. C., Worby, C. A., Simonson-Leff, N., Muda, M., Maehama, T., Hemmings, B. A. and Dixon, J. E. (2000). Use of double-stranded RNA interference in Drosophila cell lines to dissect signal transduction pathways. *Proc. Natl. Acad. Sci. USA* **97**, 6499-6503.

Costa, M., Wilson, E. T. and Wieschaus, E. (1994). A putative cell signal encoded by the folded gastrulation gene coordinates cell shape changes during Drosophila gastrulation. *Cell* **76**, 1075-1089.

Denholm, B., Brown, S., Ray, R. P., Ruiz-Gomez, M., Skaer, H. and Hombria, J. C. (2005). crossveinless-c is a RhoGAP required for actin reorganisation during morphogenesis. *Development* **132**, 2389-2400.

Fanto, M., Weber, U., Strutt, D. I. and Mlodzik, M. (2000). Nuclear signaling by Rac and Rho GTPases is required in the establishment of epithelial planar polarity in the Drosophila eye. *Curr. Biol.* **10**, 979-988.

Hacker, U. and Perrimon, N. (1998). DRhoGEF2 encodes a member of the Dbl family of oncogenes and controls cell shape changes during gastrulation in Drosophila. *Genes Dev.* **12**, 274-284.

Hu, N. and Castelli-Gair, J. (1999). Study of the posterior spiracles of Drosophila as a model to understand the genetic and cellular mechanisms controlling morphogenesis. *Dev. Biol.* **214**, 197-210.

Jaffe, A. B. and Hall, A. (2005). Rho GTPases: biochemistry and biology. *Annu. Rev. Cell Dev. Biol.* **21**, 247-269.

Karess, R. E., Chang, X. J., Edwards, K. A., Kulkarni, S., Aguilera, I. and Kiehart, D. P. (1991). The regulatory light chain of nonmuscle myosin is encoded by spaghetti-squash, a gene required for cytokinesis in Drosophila. *Cell* **65**, 1177-1189.

Kraynov, V. S., Chamberlain, C., Bokoch, G. M., Schwartz, M. A., Slabaugh, S. and Hahn, K. M. (2000). Localized Rac activation dynamics visualized in living cells. *Science* **290**, 333-337.

Lehmann, R. and Tautz, D. (1994). In situ hybridization to RNA. *Methods Cell Biol.* **44**, 575-598.

Leung, T. H., Ching, Y. P., Yam, J. W., Wong, C. M., Yau, T. O., Jin, D. Y. and Ng, I. O. (2005). Deleted in liver cancer 2 (DLC2) suppresses cell transformation by means of inhibition of RhoA activity. *Proc. Natl. Acad. Sci. USA* **102**, 15207-15212.

Lu, Y. and Settleman, J. (1999a). The Drosophila Pkn protein kinase is a Rho/Rac effector target required for dorsal closure during embryogenesis. *Genes Dev.* **13**, 1168-1180.

Luo, L., Liao, Y. J., Jan, L. Y. and Jan, Y. N. (1994). Distinct morphogenetic functions of similar small GTPases: Drosophila Drac1 is involved in axonal outgrowth and myoblast fusion. *Genes Dev.* **8**, 1787-1802.

Magie, C. R. and Parkhurst, S. M. (2005). Rho1 regulates signaling events required for proper Drosophila embryonic development. *Dev. Biol.* **278**, 144-154.

Magie, C. R., Meyer, M. R., Gorsuch, M. S. and Parkhurst, S. M. (1999). Mutations in the Rho1 small GTPase disrupt morphogenesis and segmentation during early Drosophila development. *Development* **126**, 5353-5364.

Magie, C. R., Pinto-Santini, D. and Parkhurst, S. M. (2002). Rho1 interacts with p120^{ctn} and α-catenin, and regulates cadherin-based adherens junction formation in *Drosophila*. *Development* **129**, 3771-3782.

Merabet, S., Catala, F., Pradel, J. and Graba, Y. (2002). A green fluorescent protein reporter genetic screen that identifies modifiers of Hox gene function in the Drosophila embryo. *Genetics* **162**, 189-202.

Moon, S. Y. and Zheng, Y. (2003). Rho GTPase-activating proteins in cell regulation. *Trends Cell Biol.* **13**, 13-22.

Narumiya, S., Ishizaki, T. and Watanabe, N. (1997). Rho effectors and reorganization of actin cytoskeleton. *FEBS Lett.* **410**, 68-72.

Nikolaidou, K. K. and Barrett, K. (2004). A Rho GTPase signaling pathway is used reiteratively in epithelial folding and potentially selects the outcome of Rho activation. *Curr. Biol.* **14**, 1822-1826.

Oda, H. and Tsukita, S. (1999). Dynamic features of adherens junctions during Drosophila embryonic epithelial morphogenesis revealed by a Dalpha-catenin-GFP fusion protein. *Dev. Genes Evol.* **209**, 218-225.

Oda, H. and Tsukita, S. (2001). Real-time imaging of cell-cell adherens junctions reveals that Drosophila mesoderm invagination begins with two phases of apical constriction of cells. *J. Cell Sci.* **114**, 493-501.

Padash Barmchi, M., Rogers, S. and Hacker, U. (2005). DRhoGEF2 regulates actin organization and contractility in the Drosophila blastoderm embryo. *J. Cell Biol.* **168**, 575-585.

Parks, S. and Wieschaus, E. (1991). The Drosophila gastrulation gene concertina encodes a G alpha-like protein. *Cell* **64**, 447-458.

Pilot, F. and Lecuit, T. (2005). Compartmentalized morphogenesis in epithelia: from cell to tissue shape. *Dev. Dyn.* **232**, 685-694.

Rossman, K. L., Der, C. J. and Sondek, J. (2005). GEF means go: turning on RHO GTPases with guanine nucleotide-exchange factors. *Nat. Rev. Mol. Cell Biol.* **6**, 167-180.

Royou, A., Sullivan, W. and Karess, R. (2002). Cortical recruitment of nonmuscle myosin II in early syncytial Drosophila embryos: its role in nuclear axial expansion and its regulation by Cdc2 activity. *J. Cell Biol.* **158**, 127-137.
Schneider, I. (1972). Cell lines derived from late embryonic stages of Drosophila melanogaster. *J. Embryol. Exp. Morphol.* **27**, 353-365.
Strutt, D. I., Weber, U. and Mlodzik, M. (1997). The role of RhoA in tissue polarity and Frizzled signalling. *Nature* **387**, 292-295.
Symons, M. and Settleman, J. (2000). Rho family GTPases: more than simple switches. *Trends Cell Biol.* **10**, 415-419.
Verkhusha, V. V., Tsukita, S. and Oda, H. (1999). Actin dynamics in lamellipodia of migrating border cells in the Drosophila ovary revealed by a GFP-actin fusion protein. *FEBS Lett.* **445**, 395-401.
Wong, C. M., Lee, J. M., Ching, Y. P., Jin, D. Y. and Ng, I. O. (2003). Genetic and epigenetic alterations of DLC-1 gene in hepatocellular carcinoma. *Cancer Res.* **63**, 7646-7651.
Woolner, S., Jacinto, A. and Martin, P. (2005). The small GTPase Rac plays multiple roles in epithelial sheet fusion-dynamic studies of Drosophila dorsal closure. *Dev. Biol.* **282**, 163-173.
Wu, K. Y., Hengst, U., Cox, L. J., Macosko, E. Z., Jeromin, A., Urquhart, E. R. and Jaffrey, S. R. (2005). Local translation of RhoA regulates growth cone collapse. *Nature* **436**, 1020-1024.
Young, P. E., Pesacreta, T. C. and Kiehart, D. P. (1991). Dynamic changes in the distribution of cytoplasmic myosin during Drosophila embryogenesis. *Development* **111**, 1-14.